BNL--36111

DE85 009766

Presented at Conf. on Neutrino Mass and Low Energy
Weak Interactions, Telemark Lodge, Cable, WI
Oct. 25-27, 1984

OG 827

MASTER

A Search for Neutrino Oscillations at the Brookhaven AGS

L.A. Ahrens, S.H. Aronson, P.L. Connolly*, B.G. Gibbard,
M.J. Murtagh, S.J. Murtagh, S. Terada†, and D.H. White
Physics Department, Brookhaven National Laboratory, Upton, NY 11973 C93 6000.

J.L. Callas, D. Cutts, J.S Hoftun, R.E. Lanou, and T. Shinkawa†
Department of Physics, Brown University, Providence, RI 02912 994 5000

K. Amako and S. Kabe
National Laboratory for High Energy Physics (KEK),
Ibaraki-Ken 305, Japan 930 73-0

Y. Nagashima, Y. Suzuki and S. Tatsumi
Physics Department, Osaka University, Toyanaka, Osaka 560, Japan 930 4640

K. Abe†, E.W. Beier, D.C. Doughty, L.S. Durkin, S.M. Heagy,
M. Hurley, A.K. Mann, F.M. Newcomer, H.H. Williams and T. York
Department of Physics, University of Pennsylvania,
Philadelphia, PA 19104 515 CCC0

and

D. Hedin, M.D. Marx and E. Stern
Department of Physics, State University of New York
Stony Brook, NY 11794

February 20, 1985

* Deceased
† Now at KEK

A SEARCH FOR NEUTRINO OSCILLATIONS AT THE BROOKHAVEN AGS

L.A. Ahrens, S.H. Aronson, P.L. Connolly*, B.G. Gibbard,
M.J. Murtagh, S.J. Murtagh, S. Terada†, and D.H. White
Physics Department, Brookhaven National Laboratory, Upton, NY 11973

J.L. Callas, D. Cutts, J.S Hoftun, R.E. Lanou, and T. Shinkawa†
Department of Physics, Brown University, Providence, RI 02912

K. Amako and S. Kabe
National Laboratory for High Energy Physics (KEK),
Ibaraki-Ken 305, Japan

Y. Nagashima, Y. Suzuki and S. Tatsumi
Physics Department, Osaka University, Toyanaka, Osaka 560, Japan

K. Abe†, E.W. Beier, D.C. Doughty, L.S. Durkin, S.M. Heagy,
M. Hurley, A.K. Mann, F.M. Newcomer, H.H. Williams and T. York
Department of Physics, University of Pennsylvania,
Philadelphia, PA 19104

and

D. Hedin, M.D. Marx and E. Stern
Department of Physics, State University of New York
Stony Brook, NY 11794

ABSTRACT

We report on a search for neutrino oscillations of the type $\nu_\mu \to \nu_e$ in a detector located an effective distance of 96m from the neutrino source in the wide band neutrino beam at the Brookhaven AGS. No excess of electron events was observed. The resulting upper limit on the strength of the mixing between ν_μ and ν_e in the case of large mass difference $\Delta m^2 = |m_1{}^2 - m_2{}^2|$ between the neutrino mass eigenstates m_1 and m_2 is $\sin^2 2\alpha \leq 3.4 \times 10^{-3}$ at 90% CL. The corresponding upper limit for small mass difference is $\Delta m^2 \sin 2\alpha < 0.43\ eV^2$.

INTRODUCTION

Neutrinos of a given flavor will oscillate into neutrinos of another flavor if separate lepton number is not conserved and if the neutrino flavors in question have different masses.[1] This paper reports on a search for $\nu_\mu \to \nu_e$ oscillations using the E734 detector in the wide band neutrino beam at the Brookhaven AGS. Since the neutrino source to detector distance is small ($\approx$ 96m) the experiment is most sensitive to short wavelength (high mass difference $\Delta m^2 =$

* Deceased
† Now at KEK

$|m_1^2-m_2^2|$) oscillations. No significant signal for oscillations was observed and the resulting limit on the mixing angle ($\sin^2 2\alpha$) at large Δm^2 is

$$\sin^2 2\alpha < 3.4 \times 10^{-3} \text{ at } 90\% \text{ C.L.}$$

This counter experiment result is an improvement over previous measurements in this domain which came primarily from heavy liquid bubble chamber experiments.[2]

EXPERIMENTAL DETAILS

The E734 detector was initially designed to study the elastic scattering r· ctions $\nu_\mu(\bar\nu_\mu)e^- \rightarrow \nu_\mu(\bar\nu_\mu)e^-$ and $\nu_\mu(\bar\nu_\mu)p \rightarrow \nu_\mu(\bar\nu_\mu)p$ an .o measure the quasi-elastic final states $\nu_\mu n \rightarrow \mu^- p$ and $\bar\nu_\mu p$ · n which are primarily used for normalization. It is well sui..ed for measuring low multplicity e^- final state processes such as the quasi-elastic reaction $\nu_e n \rightarrow e^- p$ which is used in this oscillation search.

The detector consists of 112 planes of liquid scintillator (each plane 4m x 4m in area x 8cm thick) and 224 planes of proportional drift cells (4.2m x 4.2m in area x 3.8 cm thick) uniformly interspersed. The fine segmentation (1,792 scintillator cells and 12,096 proportional drift cells) and the pulse height and timing characteristics of the elements provide determination of event topology, identification of electromagnetic showers, and substantial discrimination through dE/dx measurements between electrons and photons as well as pions and protons. The data used in this analysis was obtained using the wide band neutrino beam at the Brookhaven AGS for a run with 0.88×10^{19} protons on target. Data from the same run were used to determine the cross section for the reaction $\nu_\mu e^- \rightarrow \nu_\mu e^-$.[3]

DATA REDUCTION

The energy dependent flux ratio of electron neutrinos and muon neutrinos ($\Phi(E\nu_e)/\Phi(E\nu_\mu)$) was measured using the quasi-elastic reactions $\nu_e n \rightarrow e^- p$ and $\nu_\mu n \rightarrow \mu^- p$. The expected ratio for this wide band beam was calculated using a Monte Carlo program. A discrepancy between the observed and calculated ratios which has the correct energy dependence could be interpreted as evidence for $\nu_\mu \rightarrow \nu_e$ oscillations.

To obtain $e^- p$ events data from 1.25×10^6 AGS beam bursts were processed through a coarse computer based filter program[3] designed to remove events not containing a single electromagnetic shower within the angular interval $\theta_e < 240$ mrad relative to the mean neutrino beam direction. The resulting sample was scanned by physicists to eliminate events which the filter did not remove such as events with more than one electromagnetic shower or with an interacting hadron. Events with an electromagnetic shower and with associated upstream energy were retained as a control sample of photons.

The shower angle was measured by a fit to all shower hits in the proportional drift cells, and the shower energy was found by summing the deposited energy in the calorimeter cells with a correction of approximately 40% for invisible energy. The resulting angular resolution was $\Delta\theta = 30$ mrad, and the energy resolution was $\Delta E/E = 0.12/\sqrt{E(\mathrm{GeV})}$. After requiring that $0.21 < E_e < 5.1$ GeV, 873 shower events remained in the fiducial region.

There are three categories of background processes that produce forward electromagnetic showers: (a) production of π° by ν_μ-induced neutral current processes ($\nu_\mu p\pi^\circ$, $\nu_\mu n\pi^\circ$), (b) inelastic processes from ν_e interactions ($e^- p\pi^+$, $e^- n\pi^+$, $e^- p\pi^\circ$), and (c) the interaction $\nu_\mu e \to \nu_\mu e$. Reactions with a π^+ in the final state were recognized by the delayed signal from the π-μ-e decay chain. In Fig. 1a is shown the shower energy distribution of all events retained after subtraction of the π^+ background events. Most photon-induced showers from ($\nu_\mu p\pi^\circ$ and $\nu_\mu n\pi^\circ$) were recognized by their association with another significant deposition of energy or a vertex upstream of the shower. In Fig. 1b is the energy distribution of the photon-induced showers in the control sample. We expect from calculation and observation[3] that the $e^- p$ candidate sample below 0.9 GeV (Fig. 1a) contains mostly photons with a small number of electrons from $\nu_\mu e \to \nu_\mu e$, and very few electrons from $\nu_e n \to e^- p$ because of the 240 mrad cut on the shower angle. Hence it is possible to subtract the photon-induced events above 0.9 GeV in Fig. 1a by normalizing the distributions in Figs. 1a and 1b below 0.9 GeV.

There were initially 653 events in the sample with $E_e > 0.9$ GeV. Of these 20% were removed by a bin-by-bin subtraction of the π^+ events and 13% of the remaining events were removed bin-by-bin using the distribution in Fig. 1b. Further subtractions were made for the fraction of $\nu_\mu e$ events[3] (5.8%), and for energetic ($e^- p\pi^\circ$) events which by calculation amounted to 3%. The final $e^- p$ sample which contains 418 events in the region $0.9 < E_e < 5.1$ GeV is shown in Fig. 1c where comparison is made with the result of a Monte Carlo calculation.

The incident neutrino energy for the quasi-elastic ν_e events was calculated using the electron angle and energy. No direct use was made of the recoil proton since the electron algorithm selects low Q^2 events which have low energy recoil protons too short to be reconstructed as tracks in the detector.

The initial sample of ν_μ quasi-elastic candidates consisted of events which were reconstructed by the track fitting program as two-prong events. They were obtained by fully reconstructing 10% of the AGS bursts recorded on tape. It was then required that one of the prongs be identified by range and ionization[4] as a proton while the other prong exited the detector. The background in this data set when acceptances were applied consisted of charged current single π^+ production (13% of the observed $\nu_\mu n \to \mu^- p$ rate) plus a small contribution ($\approx 3\%$) from single π° and multipion events. Reactions with

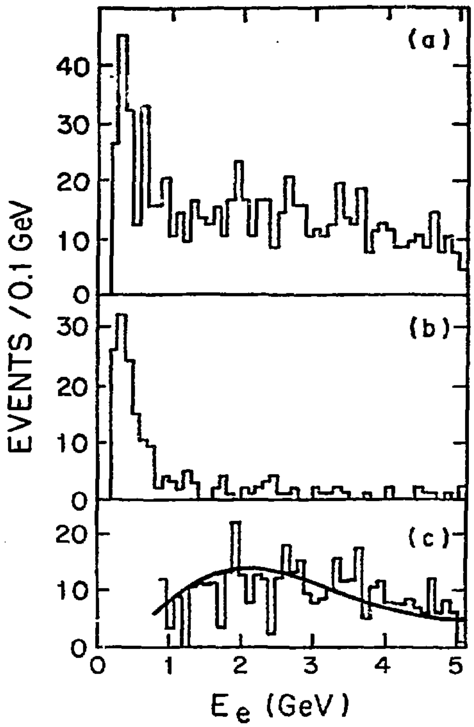

Fig. 1. (a) Shower energy distribution of all possible $\nu_e n \to e^- p$ candidate events. (b) Shower energy distribution of photons recognized as emanating from an upstream event vertex. (c) The resulting $e^- p$ energy distribution after all background subtractions. The solid line is the Monte Carlo calculated energy distribution of e^- from $\nu_e n \to e^- p$.

a π^+ were corrected for empirically using the observed events with π-μ-e decays as described in the electron analysis. The π° and multipion components were estimated by Monte Carlo calculation. The final $\mu^- p$ sample contains 1370 events.

There are many ways to determine the incident muon neutrino energy for two-prong quasi-elastic events. In this particular analysis the energy was calculated using the energy and angle of the recoil proton. It is worth noting that the Q^2 acceptance for two-prong quasi-elastics is less than for the single prong (low Q^2) quasi-elastics used for the $\nu_e n \to e^- p$ analysis. Consequently, even though the calculated flux ratio for ν_e and ν_μ is $\approx$ 1%, the combined effects of sampling to determine the ν_μ flux and the differences in acceptances gives comparable size $\nu_e n \to e^- p$ and $\nu_\mu n \to \mu^- p$ data sets in this analysis. The systematic error due to the difference in Q^2 covered by the two data sets was determined to be less than ± 14% by varying the input parameters in the ratio calculation. This error while included in the final result is not included in the errors shown in Fig. 4a.

The incident neutrino flux spectra $\phi(E(\nu_\mu))$ and $\phi(E(\nu_e))$ were obtained from the quasi-elastic data sets using Monte Carlo calculated event acceptance functions $a^{\mu p}(E)$ and $a^{ep}(E)$, the known magnitude and energy dependence of the quasi-elastic cross section[5] $\sigma_{QE}(E)$, and the measured number of protons on target (POT):

$$\phi(E(\nu_\ell)) = \frac{(\text{no. of observed QE events between E and E} + \Delta E)}{\left[\sigma_{QE}(E) \cdot a^{\ell p}(E) \cdot \Delta E \cdot \text{POT} \cdot \text{no. of tgt neutrons}\right]} \quad (1)$$

in $\nu_\ell/(\text{GeV} - \text{m}^2 - 10^{13}\ \text{POT})$, where ℓ = e or μ. The resulting spectra are shown in Figs. 2a and 2b.

It follows from the expression above for $\phi(E(\nu_\ell))$ that the flux ratio $\phi(E(\nu_e))/\phi(E(\nu_\mu))$ is given simply by the ratio of the corrected numbers of $e^- p$ and $\mu^- p$ events since the data were taken at the same time in the same beam. That ratio is shown as a function of energy in Fig. 3a. It is the ratio $\phi(E(\nu_e))/\phi(E(\nu_\mu))$ and not the absolute fluxes which must be determined reliably since it alone is used to extract the neutrino oscillation parameters.

The number of ν_e in the incident neutrino beam (due to the decays of muons and kaons) relative to the number of ν_μ in the incident beam was calculated as a function of energy using a neutrino beam Monte Carlo program[7] with the results shown as the solid lines in Figs. 2 and 3a. The agreement between the observed and calculated ν_μ and ν_e spectra in Fig. 2 is a confirmation of the validity of the beam program and of the parameters of pion and kaon production that are input to it.

The shape of $\phi(E(\nu_e))/\phi(E(\nu_\mu))$ can be understood from Table I, which gives as a function of energy the fraction of $\phi(E(\nu_e))$ and the fraction of $\phi(E(\nu_\mu))$ that arise from pions and from kaons relative to the total $\phi(E(\nu_e))$ and total $\phi(E(\nu_\mu))$. The uncertainty in $[\phi(E(\nu_e))/\phi(E(\nu_\mu))]_{calc}$ due to uncertainty in the K/π ratio-

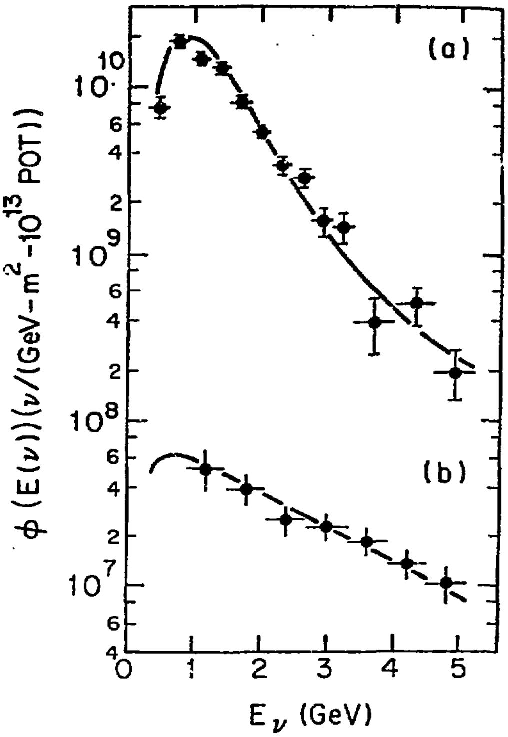

Fig. 2. (a) $\phi(E(\nu_\mu))$ obtained from the data set of $\nu_\mu n \to \mu^- p$ events. (b) $\phi(E(\nu_e))$ obtained from the data set of $\nu_e n \to e^- p$ events. The solid lines are calculated from a neutrino beam program.[7] Errors shown are statistical only. The experimental resolution in E_ν is dominated by Fermi motion of the nucleon in the target nucleus and is roughly ± 25% at E_ν = 1 GeV.

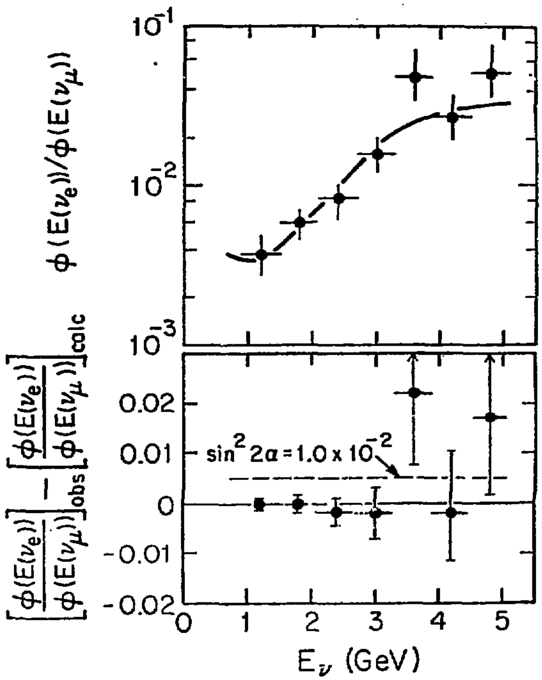

Fig. 3. (a) Plot of the flux ratio $\phi(E(\nu_e))/\phi(E(\nu_\mu))$ versus E_ν. The points represent the data while the solid line is calculated from a neutrino beam program.[7] (b) Plot of the difference between the observed and calculated flux ratios against E_ν. The dashed line is the limit on $\sin^2 2\alpha$ obtained without subtraction.

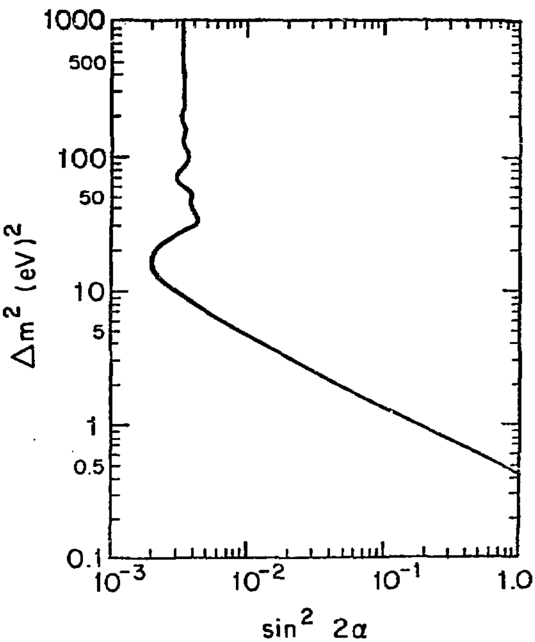

Fig. 4. The region of the $\Delta m^2 - \sin^2 2\alpha$ space excluded by this experiment.

--the sole input that quantitatively affects the flux ratio--does not exceed 15% at any neutrino energy between 1 and 5 GeV, when 20% variations are assumed in the yield of either pions or kaons (see Table I).

At $E_\nu = 1$ GeV two-thirds of $\phi(E(\nu_e))$ and 99% of $\phi(E(\nu_\mu))$ result from the π-μ-e decay chain alone. At $E_\nu = 5$ GeV, the pion and kaon roles are essentially reversed. This accounts for the relatively small variations in $\phi(E(\nu_e))/\phi(E(\nu_\mu))$ in the vicinity of those energies as the K/π ratio is varied. Furthermore, in the large Δm^2 limit, the ratio $\phi(E(\nu_e))/\phi(E(\nu_\mu))$ is independent of L/E where L is the source to detector distance, and consequently the contribution from oscillations at any energy in Fig. 3a cannot be larger than that given by the data point near 1 GeV. Hence the data at the higher energies in Fig. 3a serve as a direct test within experimental error of the accuracy of the calculation of $\phi(E(\nu_e))/\phi(E(\nu_\mu))$.

In Fig. 3b the difference between $[\phi(E(\nu_e))/\phi(E(\nu_\mu))]_{obs}$ and $[\phi(E(\nu_e))/\phi(E(\nu_\mu))]_{calc}$ is plotted as a function of E_ν. The errors shown on the data points include a systematic uncertainty of 20% (equal contributions from the acceptance functions $a^\ell P(E)$ and the flux calculation) in quadrature with the statistical uncertainties. It is clear from Fig. 3b that there is no evidence for the oscillation $\nu_\mu \rightarrow \nu_e$. Using the data between 900 and 2100 MeV, the region in the $\Delta m^2 - \sin^2 2\alpha$ space excluded with 90% confidence is shown in Fig. 4 and from this one obtains the limits

$$\sin^2 2\alpha \leq 3.4 \times 10^{-3} \text{ at 90\% C.L., in the large } \Delta m^2 \text{ limit}$$

and

$$\Delta m^2 \sin 2\alpha \leq 0.43 \text{ eV}^2 \text{ at 90\% C.L., in the small } \Delta m^2 \text{ limit.}$$

CONCLUSION

The results obtained in the experiment extend the excluded region of the $\Delta m^2 - \sin^2 2\alpha$ space for $\nu_\mu \rightarrow \nu_e$ oscillations beyond that of the previous best search[9]. In particular they improve the short wavelength limit. The results are based on the measurements of neutrino fluxes as a function of energy for a wide band beam using quasi-elastic events. This ability to measure spectra with a highly segmented calorimetric detector is encouraging for future oscillation searches since it may enable one to use the high fluxes only available in wide band beams to do precision searches.

This work was supported in part by the U.S. Department of Energy, the Japanese Ministry of Education, Science and Culture through the Japan-USA Cooperative Research Project on High Energy Physics, the U.S. National Science Foundation and the Stony Brook Incentive Fund.

Table I. An example of the relative kaon contributions $R_e^K \equiv \phi(\nu_e(K))/\phi(\nu_e(\text{all}))$ and $R_\mu^K \equiv \phi(\nu_\mu(K))/\phi(\nu_\mu(\text{all}))$ to the total fluxes $\phi(E(\nu_e))$ and $\phi(E(\nu_\mu))$, respectively, is given in columns 2 and 3. Relative pion contributions are $(1-R_e^K)$ and $(1-R_\mu^K)$. The last two columns exhibit the variation in $\phi(E(\nu_e))/\phi(E(\nu_\mu)) = [1-R_e^K(1-r)]/[1-R_\mu^K(1-r)]$ for 20% changes in the value of r, the ratio of the kaon to pion yields integrated over contributing meson momenta. The normalization is arranged to give $\phi(E(\nu_e))/\phi(E(\nu_\mu)) = 1.00$ for $r = 1.0$.

Energy GeV	R_e^K	R_μ^K	$\phi(E(\nu_e))/\phi(E(\nu_\mu))$	
			$r = 1.2$	$r = 0.8$
1	0.34	0.006	1.07	0.94
2	0.68	0.013	1.113	0.89
3	0.85	0.10	1.15	0.87
4	0.90	0.36	1.10	0.90
5	0.94	0.67	1.05	0.95

REFERENCES

* Deceased.

† Now at KEK.

1. For reviews of neutrino oscillations, see, e.g., A.K. Mann and H. Primakoff, Phys. Rev. D15, 655 (1977); S.M. Bilenky and B. Ponetcorvo, Phys. Repts. 41, 225 (1978).
2. For a recent summary of the status of neutrino mass and mixing experiments, see M.H. Shaevitz, Proc. 1983 International Symposium on Lepton and Photon Interactions at High Energies, Ed. D.G. Cassel and D.L. Kreinick, Cornell University, Ithaca, NY (p. 132).
3. L.A. Ahrens et al., Phys. Rev. Lett. 51, 1514 (1983); L.A. Ahrens et al., Phys. Rev. Lett. 54, 18 (1985).
4. D.C. Doughty Jr., A Measurement of Neutrino-Proton Elastic Scattering, Ph.D Thesis, University of Pennsylvania, December 1983 (unpublished).
5. N.J. Baker et al. Phys. Rev. D25, 2495 (1981).
6. The effective neutrino source to detector distance is calculated as follows. The distance from the target on which protons from the AGS impinge to the end of the meson decay region is 61.7 m, along which meson decays occur almost uniformly. The distance from the end of the decay region to the middle of the detector is 65.6 m. Hence, adding one-half the length of the decay region to 65.6 m yields 96.4 m.
7. The beam program used was a CERN wide band beam program (Hydra Applications Library, Nubeam: Neutrino Beam Simulator, C. Visser, CERN, 1979) modified extensively by R.D. Carlini, Los Alamos National Laboratory. The systematics of pion and kaon production used to obtain the curves in Figs. 2 and 3a were based on the semi-empirical studies cited in reference 8. The two studies give for r, the K^+/π^+ ratio averaged overall meson momenta from 1 to 14 GeV/c, 0.083 (GHR) and 0.089 (SW). In either study variations in the ratio $\phi(E(\nu_e))/\phi(E(\nu_\mu))$ at any E_ν between 1 and 5 GeV due to ± 20% variations in r differ by less than 15% from the values of $\phi(E(\nu_e))/\phi(E(\nu_\mu))$ obtained for r at its central value in that study (see Table I). Details of this work on neutrino beams at BNL are in D.H. White, BNL internal report OG793, and will be published elsewhere.
8. J.R. Sanford and C.L. Wang, BNL 11479, 1967 (unpublished), and H. Grote, R. Hagedorn and J. Ranft, Particle Spectra, CERN, 1979 (unpublished).
9. N.J. Baker et al., Phys. Rev. Lett. 47, 1576 (1981).